A COMPARISON BETWEEN 'ASTER' ALTERATION ANOMALIES AND STRUCTURAL MAPPING AT OORAMINNA, WATERHOUSE, JOHNSTONE/GYPSUM AND Mt. KITTY.

Memorandum prepared for
Central Petroleum Ltd.
By R. Russell
5th December 2006

1 INTRODUCTION

1.1 Background

Alteration styles and mineralisation at the surface of the Palm Valley gas field were imaged by Geoscan airborne AMSS MkII instrument. Patterns related to seeping hydrocarbons were located and interpreted by R. Agar (1999). Attempts have been made by AGARSS Pty. Ltd. to map the same alteration styles and minerals over Central Petroleum's four Amadeus Basin prospects, Ooraminna, Waterhouse, Mt. Kitty and Johnstone. A report detailing this work has been prepared by R. Agar (Agar, 2006).

1.2 Central Petroleum Prospects

The present work is based on ASTER space imagery which has a resolution of 30m as opposed to 9m for the airborne imagery. This is given as the main reason for the partial lack of success of this work in the four areas studied (Agar, 2006). Neither the lithology's nor the individual alteration minerals identified at Palm Valley could be consistently distinguished in the four Central Petroleum's prospects.

However, similar colour anomalies to those at Palm Valley can be detected in the ASTER imagery and their cause has been attributed to similar alteration effects. The most striking alteration effects are at Ooraminna where there is a strong correlation between the FeOx and FeOH enrichment, AlOH depletion and positive temperature anomalism. It is possible that active hydrocarbon seepage is occurring at this prospect.

Elsewhere, the anomalism is less prominent. Temperature does not reliably coincide with alteration styles of FeOx, FeOH and AlOH. It is possible that positive temperature anomalism may be associated with active seepages while the lack of temperature differences may mean that the seepage has become inactive.

1.3 The Report

It is the intention of this memorandum to compare and evaluate the alteration targets outlined by AGARSS (Agar, 2006) with the structural mapping completed by the writer in November 2006 (Russell, 2006).

2 CONCLUSIONS

2.1 Ooraminna

Seven alteration anomalies are identified from the ASTER data on the Ooraminna Anticline (Agar, 2006). The most significant of the anomalies are considered to be 1, 2, 3 and 5. They are situated near the culmination and western plunging nose of the anticline. The anomalies have a similar pattern to those imaged at Palm Valley and suggest that active hydrocarbon seepage is occurring from a significant hydrocarbon reservoir on the western nose and culmination of the Ooraminna Anticline.

Ooraminna ASTER anomaly 1 is the strongest in all the Amadeus Basin project areas. The location of the anomaly suggests that hydrocarbons are seeping from the spill-point of a hydrocarbon reservoir on the western nose of the anticline. A large area with high fracture density and fracture intersection zones has been mapped from the air photographs immediately to the south of Anomaly 1 along the crest of the anticline (zones O^2 and O^3, Russell, 2006). The writer interprets the coincidence of these anomalous zones as highly significant. In particular, the culmination of the fold immediately south of anomaly 1 in the vicinity of the O^2 high fracture zone should be the focus for future exploration.

Further, less intense alteration and temperature anomalies on the culmination of the Ooraminna fold and further down-dip on the western nose of the structure indicate that seepage may also be occurring here. The fracture density is not as high in these areas so the prospectivity is accordingly rated as lower. Nevertheless, these zones are thought to be highly significant for hydrocarbon exploration.

2.2 Waterhouse

Eight alteration anomalies are identified from the ASTER data over the Waterhouse Anticline (Agar, 2006). The largest and most significant is Waterhouse 1 which covers most of the plunging western nose of the fold. The anomaly comprises all the major alteration features including a positive temperature anomaly and coincides closely with the highly rated 'W^1' fracture zone mapped from air photographs (Russell, 2006). A possible drawback is the structural complexity of this western nose where the crest of the fold is sliced by a series of thrust or reverse faults.

The Waterhouse 7 anomaly covers a large part of the crestal and eastern part of the fold. The eastern end of anomaly 7 is strongly anomalous and coincides with the W^4 high fracture zone. The coincidence of the strong alteration with the high fracture zone at W^4 is regarded by the writer as highly significant.

Both the W^1 and W^4 areas should be the focus of further exploration at Waterhouse.

2.3 Johnstone/Gypsum

19 alteration zones are identified from the ASTER imagery at the Johnstone/Gypsum prospect (Agar, 2006). The area is strongly overprinted by aeolian and evaporite deposits which makes interpretation of the anomalies difficult.. The high number of ASTER anomalies in places where there is thought to be little chance of hydrocarbon seepage suggests that other factors are affecting the surface mineralogy. Only 4 of the anomalies actually lie within or close to the areas of specific interest and none are regarded as particularly significant.

2.4 Mt Kitty

9 anomalies are identified from the ASTER imagery (Agar, 2006). Three are located in, or in close proximity to, the interpreted basement high which represents the hydrocarbon target in this area. The region is strongly overprinted by transported surface materials and claypans which make the anomalies difficult to evaluate. Most of them appear to reflect the underlying geomorphology rather than deeper structures. The three important anomalies are considered to be Mt. Kitty 1, 6 and 7.

Mt. Kitty ASTER anomaly 1 covers a large area on the southern flank of the hydrocarbon prospect. It appears to lie on a major fracture intersection zone. The writer considers that the anomaly is more likely to be related to the geomorphology than to seepage of hydrocarbons. The Mt. Kitty 6 and 7 anomalies are located close to the northwestern boundary of the Mt. Kitty basement high. The writer considers the anomalies to be significant but not conclusive evidence of hydrocarbon seepage.

3 COMPARISON OF 'ASTER' ANOMALIES WITH STRUCTURE

3.1 OORAMINNA

3.1.1 'Ooraminna 1' Anomaly

Seven alteration anomalies are identified from the ASTER data on the Ooraminna Anticline (Agar, 2006). The largest and most prominent anomaly is designated as 'Ooraminna 1'. This anomaly lies along the northern flank of the western plunging nose of the structure. At its eastern end, the anomaly extends southward to cover the crest of the anticline immediately south of the Ooraminna 1 well (Agar, 2006 p14). The anomaly cross-cuts the Arumbera Sandstone, the Todd River Dolomite and extends down-dip into the Giles Creek Dolomite. The main part of the anomaly does not coincide with the crest of the structure. At Palm Valley, a similar pattern was noted. That is, the alteration at the surface was not exactly coincident with the position of the gas field for reasons that were unclear.

The alteration anomaly enhances the prospectivity of the structural targets mapped from the air photographs at O^2 and O^3. It is not clear why the apparent seepage is mainly on the northern flank of the anticline rather than the crest. The anomaly could represent the spill point of the reservoir and the seal at the crest may be highly effective. But this does not explain the lack of an anomaly on the southern flank of the anticline. However, the experience at Palm Valley suggests that this is probably not important. The evidence is that there is possibly a major active hydrocarbon seep on the western nose of the Ooraminna anticline close to where the best fracture porosity has been predicted from the air photograph mapping. In the writers opinion, this coincidence is highly significant and the area should be a major focus for Central Petroleum's future exploration effort.

3.1.2 'Ooraminna 2' and '3' Anomalies

A small alteration and temperature anomaly is identified at 'Ooraminna 2' on the southern flank of the anticline in the Arumbera Sandstone. This zone has the same signature as Ooraminna 1 and is located to the south of the main culmination of the anticline. The 'Ooraminna 3' anomaly is an arcuate alteration zone which extends from 'Ooraminna 2', across the culmination of the anticline, to link with 'Ooraminna 1'. There is no temperature anomaly at 'Ooraminna 3'. Thus, the whole crestal area of the anticline in the vicinity of the regional culmination appears to be anomalous with stronger alteration and relatively high temperature on the southern flank. The minor high fracture zone mapped from the air photographs at O^4 is thus enhanced by the alteration pattern.

3.1.3 'Ooraminna 5'

FeOx and FeOH enrichment and a negative temperature anomaly is mapped at 'Ooraminna 5' on the western plunging nose of the anticline. This anomaly coincides with the outcrop of the Giles Creek Dolomite. The air photograph mapping shows a coincident fracture reservoir target (O^1, Russell 2006). This coincidence between the alteration target and the fracture density target thus enhances the prospectivity of the area.

3.1.4 Ooraminna '4' to '7' Anomalies.

The rest of the alteration anomalies outlined by R. Agar (2006, anomalies 4 to 7) do not coincide with highly fractured zones identified from the air photograph mapping. This is not to say that they are not prospective for hydrocarbons. Rather, it is less likely that any associated hydrocarbon reservoir will have significant fracture porosity.

3.2 Waterhouse

3.2.1 'Waterhouse 1' Anomaly

Eight alteration anomalies are identified from the ASTER data over the Waterhouse Anticline (Agar, 2006). The largest and probably the most significant is Waterhouse 1 which covers most of the plunging western nose of the fold. The anomaly comprises all the major alteration features including a positive temperature anomaly. It coincides closely with the 'W1' fracture zone mapped from air photographs (Russell, 2006) which is highly rated. The only drawback of this anomaly is the structural complexity of this western nose where the crest of the fold is sliced by a series of thrust or reverse faults.

3.2.2 'Waterhouse 7' anomaly

The Waterhouse 7 anomaly covers a large part of the crestal and eastern part of the fold. This is essentially the outcrop area of the Goyder and Jay Creek Formations. The central part of the fold is cylindrical and is not regarded as highly fractured. However, the eastern nose of the anticline is considerably fractured and two significant fracture targets are mapped here (W^3 and W^4, Russell 2006). The eastern end of Anomaly 7 is strongly anomalous on the ASTER and coincides with the W^4 high fracture zone. The W^3 fracture zone to the west of W^4 is not anomalous on the ASTER.

3.2.3 Other Waterhouse anomalies

The other anomalies at Waterhouse are strata-bound and lie on the limbs of the fold. None of them coincide with high fracture zones. The strongest of the anomalies is number 8, located along the northern flank of the anticline with FeOx and FeOH enrichment coupled with AlOH depletion and a positive temperature anomaly. Apart from Waterhouse 3, all the anomalies are in low fracture density areas in the cylindrical part of the fold. At 3, the sandstones are bleached on the east plunging nose of the anticline but there is no mineral enrichment and no temperature anomaly.

3.3 Johnstone/Gypsum

19 alteration zones are identified from the ASTER imagery in the Johnstone/Gypsum area (Agar, 2006). The sand dunes which cover the area can be clearly seen on the

images. However, the inter-dune areas show variability in the alteration and temperature patterns. None of the anomalies outlined from the ASTER can conclusively be related to what are thought to be the hydrocarbon prospects at Johnstone and Gypsum. The high number of anomalies in places where there is thought to be little likelihood of hydrocarbon seepage suggests that other factors are affecting the surface mineralogy.

The area analysed on the ASTER is much larger than the actual area of the Johnstone and Gypsum prospects so only 4 of the anomalies actually lie within or close to the areas of specific interest. They are Anomalies 4, 6, 7 and 15. These are of particular interest here.

3.3.1 Johnstone 15

The Johnstone 15 anomaly is a relatively small area of enriched Fe and depleted AlOH in a low temperature zone. The anomaly has a moderate to weak signature and it coincides with the western end of the Johnstone target. It is located in area of good outcrop and the writer thinks that this is possibly the overriding reason for the anomaly on the ASTER. Nevertheless, it could represent a spill-point seep from a hydrocarbon reservoir which is situated to the east.

3.3.2 Johnstone 6 and 7

Johnstone 7 occupies a position on the eastern end of the Johnstone prospect and contains strong FeOx and FeOH enrichment with AlOH depletion. The temperature is neutral. The anomaly lies in the floor of an old north-south trending claypan that has been filled with aeolian sands. It is possible that the alteration could reflect a colluvial or alluvial dump zone in the claypan system. However, as at Johnstone 15, it could also represent a spill-point seep from a hydrocarbon reservoir on the crest of the prospect to the west.

Johnstone 6 occupies a similar geomorphological position a little to the south of 7 in the old claypan. The anomaly lies to the southeast of Johnstone and west of Gypsum. The anomaly is similar to 7 except that the temperature is negative. Again, it is possible that the alteration could reflect a colluvial or alluvial dump zone in the claypan system.

3.3.3 Johnstone 4

This anomaly is an area of strong FeOx and FeOH enrichment with AlOH depletion. The temperature is neutral. It lies near the eastern end of the Gypsum 1 target and may represent a seep from a reservoir in the culmination to the west. However, it is possible that the anomalous surface patterns could be related to the geomorphology. The anomaly is partly situated over a palaeo-claypan.

3.4 Mt. Kitty

9 anomalies are identified from the ASTER imagery at Mt. Kitty (Agar, 2006). Three are located in, or in close proximity to, the interpreted basement high which represents the hydrocarbon target in this area. The region is strongly overprinted by transported surface

materials and claypans which make the anomalies difficult to evaluate. Most of them appear to reflect the underlying geomorphology rather than deeper structures.

The three important anomalies are considered to be Mt. Kitty 1, 6 and 7.

3.4.1 Mt. Kitty 1

Mt. Kitty 1 covers a large area on the southern flank of the hydrocarbon prospect. It appears to lie on a major fracture intersection zone. The primary fracture trend is north-northwest while secondary trends are to the northwest and northeast. The secondary trends are not obvious on the air photographs. It is possible that the northeastern trend is a basement fault controlling the southeastern flank of the Mt Kitty basement high. The strong north-northwest trend appears to partly form the eastern termination of the structural high. The anomaly is enriched in iron and depleted in AlOH with a complex temperature pattern. A north-northwest trending palaeochannel is mapped through the area which coincides with the main fracture and a low temperature linear. The writer considers that the anomaly is much more likely to be related to the geomorphology than seepage of hydrocarbons.

3.4.2 Mt. Kitty 6 and 7

The Mt. Kitty 6 and 7 anomalies are located close to the northwestern boundary of the Mt. Kitty basement high. Both have FeOx and FeOH enrichment in a positive temperature area. They are located on low angle gibber slopes extending from palaeo land surface remnants down to claypans. The area is crossed by northeast trending faults which may control the northwestern edge of the Mt. Kitty basement high. It is possible that hydrocarbons could be seeping through the Gillen Salt seal along the faults in this location. The anomalies are not strong but then, they are not expected to be in this environment. The writer considers the anomalies to be significant but not conclusive evidence of hydrocarbon seepage.

4 REFERENCES

Agar, R.A., 1999 — *Spectral and Mineralogical Characterisation of Alteration Associated with Hydrocarbon Seepage Using Geoscan AMSS MKII Data over Palm Valley, Australia.* Pro. Of 13th Intl. Conf. On Applied Geologic Remote Sensing; Vancouver, B.C. Canada, March 1999; ERIM, Ann Arbor, Michigan, USA.

Agar, R.A., 2006 — *ASTER Alteration Mineral Mapping for Hydrocarbon Seepages; Waterhouse, Ooraminna, Johnston and Mt. Kitty Areas, Amadeus Basin, Central Australia.* Unpub. Report for Central Petroleum Ltd., November, 22pp.

Russell, R., 2006 — *Air Photograph Mapping of Fracture Patterns and Other Structures of the Johnstone/Gypsum, Mt. Kitty, Ooraminna and Waterhouse Projects, Amadeus Basin.* Unpub Report, Central Petroleum Ltd, November, 11pp.

AIR PHOTOGRAPH MAPPING OF FRACTURE PATTERNS AND OTHER STRUCTURES OF THE

JOHNSTONE/GYPSUM, MT KITTY, OORAMINNA AND WATERHOUSE PROJECTS, AMADEUS BASIN

Report by R. Russell
Central Petroleum Ltd
November 2006

CONTENTS

LIST OF TABLES

LIST OF FIGURES

ENCLOSURES

1 INTRODUCTION

1.1 Brief

Air photograph interpretation has been carried out over four of Central Petroleum's hydrocarbon prospects in the Amadeus Basin. The four prospects are Johnstone/Gypsum, Mt. Kitty, Ooraminna and Waterhouse. The main purpose of the mapping is to locate fractures and other structural features on, or close to the prospective structures.

At Ooraminna and Waterhouse, the intersection zones between different fracture sets are likely to represent locations where better reservoir potential for hydrocarbons occurs at depth. The structural patterns on the two anticlines are analysed here to locate zones where fracturing is likely to be at a maximum.

The mapping at Johnstone/Gypsum and Mt. Kitty is more general. The intention of the work is to locate structures which may relate to the hydrocarbon traps thought to exist at depth. The structures and concepts mapped from the air photographs can then be factored-in to the model of the targets and used in the planning of seismic lines.

1.2 Data

The mapping is based on stereo air photographs.

At Mount Kitty and Johnstone/Gypsum, black and white photographs were used at a scale of about 1:80,000. The photography dates from 1984 and 1985. The quality of the imagery is regarded as moderate to good.

For the Ooraminna and Waterhouse projects, colour air photography at a scale of 1:25,000 was flown specifically for this work in May, 2006. This imagery is excellent.

Landsat TM imagery was also obtained covering the project areas. Treatments of bands 531 (RGB) were produced over the project areas. However, it was decided to use more sophisticated spectral analysis of the Landsat to support the air photograph mapping. Dr. R. Agar is carrying out this work at the time of writing. The results will be contained in a separate report.

1.3 Maps

The photo-interpretations of the project areas are presented in this report as neat pencil-drawn maps. For convenience, the Ooraminna and Waterhouse maps are produced at a scale of 1:50,000 (Enclosures 1 and 2) while the Johnstone/Gypsum and Mt. Kitty maps are at 1:100,000 (Enclosures 3 and 4).

1.4 Technique

The usual techniques of air photograph interpretation were used in the mapping. Outcrop geology was mapped from photo tones and textures in conjunction with the geomorphology. Faults were interpreted from linear features. These may be vegetation patterns, breaks or horizontal displacements in the stratigraphy and geomorphological features.

The resulting maps represent uncontrolled photo-mosaics. The maps suffer from the same altitude and radial distortions as the original air photographs. However, the project areas have relatively low relief in relation their size and the distortions are regarded as acceptable within the context of this project.

1.5 Conclusions

1.5.1 Johnstone/Gypsum

The main hydrocarbon prospect at Johnstone is a hanging wall closure on a southerly dipping thrust fault. Other plays are identified to the southeast of Johnstone at Gypsum 1 and 2. The major thrust faults at Johnstone and Gypsum cannot be seen on the air photographs probably due to the strong aeolian and evaprorite overprint. However, major northeast trending faults are mapped in the area between Johnstone and Gypsum. These faults could represent relay-type faults which separate the two prospects.

Closure at the Gypsum 2 prospect may be larger than previously mapped. The prospect could extend southeastward into an area where the seismic data is very poor. Here, a west-northwest trending faulted high runs into an anticline comprising Early Palaeozoic units. The faults cannot be seen on the air photographs and the rock types and dips on the anticline are difficult to identify. This area would benefit from field mapping to locate both the culmination of the fold structure and the faults which may control the west-northwest trending structural high.

1.5.2 Mt. Kitty

The Mt. Kitty prospect is a basement high overlain by Heavitree Quartzite, Bitter Springs Formation and Cambrian sediments. Part of the Bitter Springs Formation is the Gillen Salt Member which is thought to attain considerable thickness at Mt. Kitty and provide a seal for the trap. It is therefore thought to be unlikely that much of the basement faulting will extend to the surface through the salt. The faults mapped from the air photographs may be relatively shallow structures, only penetrating the Palaeozoic units overlying the Gillen salt.

1.5.3 Ooraminna

A total of five highly fractured 'sweet spots' are identified from the air photograph mapping in the crestal region of the anticline. The targets occur in two main prospective zones. They are:

- The sinusoidal **crest of the fold** to the east of Ooraminna 1. *Two* relatively small fracture intersection zones are mapped here.
- The **western plunging nose** of the fold. *Three* zones of high fracturing are identified. The central zone is the largest and contains the highest frequency of fractures. The other two zones are less fractured.

1.5.4 Waterhouse

The air photograph mapping suggests that the two plunging noses of the structure represent the best targets for fracture-porosity reservoirs.

- The prospective area on the **western** nose is about 15 kilometres long and 4 kilometres wide. *Two* main high fracture zones are identified here. The two zones may actually represent a single high fracture zone as the area in between them comprises outcropping shale which tends to obscure the traces of the faults on the air photographs.
- The prospects on the **eastern** plunging nose are thought to be even better than the western nose. *Two* fracture intersection zones are identified. The first contains the highest fracture densities on the anticline comprising two intersecting sets while the second is further up the crest of the structure and is less fractured.

A further four fracture intersection zones are mapped in the cylindrical central section of the fold which are not thought to be as prospective as the four targets on the plunging noses of the fold.

2 GEOLOGICAL BACKGROUND

2.1 Fracture types

Three main types of fracture have been identified in anticlinal structures of the Amadeus Basin. They are:

- **Syn-tectonic thrust and reverse faults** which trend parallel to the fold axes. These faults are compressional brittle failures usually produced along the axis or on the flank of a fold structure during the orogeny which formed the folds.

- The second fracture sets trend at right angles or sub-perpendicular to the folding. These are shorter extensional fault elements and are produced by **erosional unloading**. Individually, the two fault sets do not necessarily interconnect. However, where both sets occur in the same area, there is much more likely to be interconnection and fracture porosity becomes probable.

- In addition, the zones of maximum curvature along anticlinal and also possibly synclinal axes are commonly the locations of **radial extension fracturing**. This 'Gaussian curvature' is though to be significant when assessing the likelihood of fracture porosity.

2.2 Other Structural Factors Controlling Fracture Density

Cylindrical folds tend to produce limited fracture densities. However, where the axis of the fold is **plunging** or where it deviates in any direction, an increase in fracture density usually occurs. A dome would therefore be more prospective for fracture porosity than a cylindrical fold. The difference in fracture porosity between Palm Valley, a dome-like fold where the reservoir is fracture controlled, and Mereenie, a cylindrical fold where fracture porosity is insignificant, are examples of this process.

2.3 Summary

In summary, high fracture porosity appears to be associated with:

1 **Intersecting sets** of thrust/reverse faults trending parallel to the fold axes and extension faults at right angles to the folds.
2 Zones of maximum **curvature** along the fold axes.
3 **Plunging or deviation** in the axes of the folds

These principles are applied to the air photograph mapping in the prospect areas.

3 MAPS

3.1 Johnstone/Gypsum

3.1.1 Geomorphology and Outcrop

The photo geology of the Johnstone and Gypsum project area is shown as Enclosure 1. The area is overprinted by an extensive aeolian sand sheet which has been worked by the wind into longitudinal dunes trending east-northeast. In the central parts of the mapped area are large claypans which represent a regional topographic sink.

Areas of gibber (rocky armoured gravel plains) probably represent outcropping or subcropping stratigraphic units. A broad belt of gibber extends roughly northeast to southwest across the mapped area. The best rock outcrops occur in the northwest of the map. Here, a salt diapir has intruded a thick pile of Palaeozoic strata which dip steeply to the south.

3.1.2 Faults

Photo linears have been mapped which are thought to be major unconformities or faults in the bedrock. A major lineation trends west-northwest to the north of the salt diapir. This feature is interpreted as a major unconformity in the steeply dipping Palaeozoic units. Other lineations trend northeast or northwest. These features may represent conjugate faults generated during the Alice Springs Orogeny.

3.1.3 Hydrocarbon Targets in relation to air photo mapping

The main hydrocarbon prospect at Johnstone is a hanging wall closure on a southerly dipping thrust fault. Other plays are identified to the southeast at Gypsum 1 and 2. The Johnstone and Gypsum prospects are outlined on Enclosure 1. The major thrust fault at Johnstone cannot be seen on the air photographs. There is also little correlation between the Gypsum targets and the photo mapping. The aeolian overprint is clearly too strong for the underlying geology to show through to the surface.

However, major northeast trending faults are mapped in the area between Johnstone and Gypsum. These could represent relay-type faults which have divided the folding stresses in the two areas.

Immediately to the southeast of Gypsum 1 prospect, seismic data is very poor in the vicinity of a possible anticlinal culmination. The culmination appears to be fault-bounded and could extend the theoretical area of closure of the prospect considerably. The air photograph mapping shows relatively reasonable outcrop in this area with the two limbs of the anticline converging to the west (A, Enclosure 1). The faults cannot be seen and the rock types and dips are difficult to identify. The area would benefit from field mapping to locate the possible culmination of the structure and any faults which may significantly affect it.

3.2 Mt. Kitty

3.2.1 Geomorphology and outcrop

The Mt. Kitty mapping is presented here as Enclosure 2. The area comprises a broad aeolian sand sheet in the southwest which rests on an old land surface. The surface is being eroded to the northeast by Recent fluvial erosion. A breakaway marks the edge of the old surface. Northward flowing creeks and broad saltpans occur in the eroding area.

3.2.2 Faults

Strong linear segments of geomorphology can be seen on the air photographs which are interpreted as possible faults. The dominant trends are north-northwest and northeast. Strong linear trends to the west-northwest are interpreted as bedding planes in the outcropping Palaeozoic units.

3.2.3 Hydrocarbon targets in relation to air photo mapping

The Mt. Kitty prospect is a basement high overlain by Heavitree Quartzite and the Bitter Springs Formation. The basement high is outlined on Enclosure 2. Part of the Bitter Springs Formation is the Gillen Salt Member which is thought to attain considerable thickness at Mt. Kitty. It is therefore thought to be unlikely that much of the basement faulting will extend to the surface through the salt. The faults mapped from the air photographs are therefore likely to be relatively shallow structures, only penetrating the Palaeozoic units overlying the Gillen salt. Indeed, the photo mapping does not appear to show any of the features of the basement high. Nevertheless, the mapped fault pattern will be useful when interpreting the seismic data.

3.3 Ooraminna

3.3.1 Geomorphology and structure

The Ooraminna anticline is located some 130 kilometres east of Palm Valley in the northeastern Amadeus Basin. The axis of the structure runs approximately east-northeast/west-southwest. The dominant plunge is to the west-southwest. The air photograph mapping (Enclosure 3) shows that plunge is also possible to the east. On the photo mapping, the culmination appears to be located about 4 kilometres east-southeast of the Ooraminna 1 well. The present mapping suggests that the well was not drilled on the crest of the fold.

The crestal part of the structure is rugged and comprises deeply incised gullies cut into the Arumbera Sandstone and Todd River Dolomite. A major south-flowing creek has cut through the centre of the structure. It is likely that the creek has been superimposed from an earlier land surface (possibly of Cretaceous-age) and has maintained its course as the land surface was lowered by erosion.

3.3.2 Faults

Numerous photo linears have been mapped from the air photographs. Most of these are thought to be faults. However, some of the longer, curved linears may be major unconformities. An example occurs about 3 kilometres to the northeast of Ooraminna 1 where the Todd River Dolomite contacts with the Arumbera Sandstone.

Most of the faulting is parallel to the crest of the anticline and occurs on the southwestern plunging nose of the structure. These faults are interpreted as thrust and reverse faults which formed at the same time as the folding. This group of faults extend eastward towards the central parts of the fold. They appear to become obscure adjacent to Ooraminna 1. The fold-parallel faults then re-appear on the northern flank of the structure further east and merge with a strong northeast trending fault zone in the northeast of the mapped area.

Other faults occur on different trends in the mapped area. Many of them are on the flanks of the structure and do not reach the prospective crestal area. In the east, the main faults are interpreted as 'X' and 'R' conjugate shears related to the folding. Other smaller faults are probably normal dilational faults related to erosional unloading. These faults are highly significant when they occur on the crest of the fold.

3.3.3 High-grade areas for fracture porosity

The most likely areas for high fracture porosity in the Ooraminna Anticline are thought to be where three structural features coincide. They are:

- The intersection zones between syn-tectonic thrust/reverse faults along the crest of the fold and faults at approximately right angles to the fold caused by erosional unloading.
- The zone of high 'Gaussian' strain along the crest of the fold where the folded beds are changing dip.
- The zones of increased fracturing due to non-cylindrical folding.

Zones where these three features coincide are shown on Enclosure 3. Two main areas are high-graded. They are:

1 The first is the sinusoidal **crest of the fold** to the east of Ooraminna 1. This is interpreted as a zone of non-cylindrical folding. At the centre of the area, the axis of the fold deviates from almost east-west to northeast. The potential for radial compressional and extensional fracturing is therefore enhanced. However, there is not a high frequency of fractures mapped from the air photographs. Two relatively small fracture intersection zones are mapped. The first is close to the interpreted culmination of the structure and the second is on the northern flank.
2 The second high-grade area is the **western plunging nose** of the fold. The fold plunges to the southwest and this zone of non-cylindrical folding appears to be relatively highly faulted on the air photographs. Three zones of high fracturing are

identified. The central zone is the largest and contains the highest frequency of fractures. The other two zones are less fractured.

The five high fracture zones on the crestal and western nose of the anticline are listed and ranked on Table 1. The Ooraminna 1 well is located outside of the area of interest. The reasons for this are not fully understood by the writer. The well was located using seismic and air photograph mapping. On the present air photographs, the crest of the fold is quite clear and occurs about 1.5km to the south of the well site. The present mapping suggests that if the well had been drilled on-structure, a much more positive result would have been obtained.

Table 1 Fracture reservoir targets, Ooraminna Anticline.

TARGET (See Enc. 3)	RANK	COMMENTS
O^2	1	Central high fracture zone, Western Nose. High frequency of fractures parallel to the fold crest and at right angles. The best target zone on the air photo map.
O^1	2	Western high fracture zone, Western Nose. Fault intersections caused by splays on the thrust/reverse fault trend. Transverse faults crossing the fold are absent.
O^5	3	Northern flank, Crestal area. North-northeast trending faults intersect with a northwest trending fault. The target zone is on the northern flank of the fold
O^3	4	Eastern high fracture zone, Western Nose. A single north-south fault crosses the crest of the anticline.
O^4	5	Crestal zone. Minor fracture intersection. Major regional culmination seen as a positive feature

3.4 Waterhouse

3.4.1 Geomorphology and structure

The Waterhouse anticline is located about 65 kilometres east of Palm Valley in the northern Amadeus Basin. The fold is a double plunging, tightly folded structure with an outcrop area about 50 kilometres long and 8 kilometres wide. The axis of the structure runs approximately east-west. The eastern and western ends of the fold plunge to the west-northwest and east-northeast respectively. However, the main part of the fold is approximately cylindrical. On the photo mapping (Enclosure 4), the crest of the fold does not appear to be straight but deviates slightly. This may suggest that the axis of the structure dips slightly, probably to the north.

Shales and dolomitic shale of the Goyder Formation and Jay Creek Limestone are exposed along the crest of the fold. These easily eroded units have formed low ground in the centre of the structure. The Pacoota Sandstone, Horn Valley Siltstone, Mereenie Sandstone and Hermansburg Sandstone form the rest of the outcropping units in the fold. These are much more resistant units and they form a high 'wall' encircling the low-lying centre of the structure. This 'wall' of resistant rocks forms rugged topography incised by steep gorges. As at Ooraminna, a major south-flowing creek has cut through the centre of the structure. This creek is likely to have been superimposed on the fold in the same way.

3.4.2 Faults

Numerous photo linears have been mapped from the air photographs. Most of these are interpreted as faults.

The fault patterns on the western and eastern plunging noses of the anticline are different and probably reflect different structural controls.

- The *western* nose contains a high frequency of major faults running parallel to the crest of the anticline. These faults are interpreted as thrust and reverse faults which formed at the same time as the folding. This group of faults appears to extend eastward only as far as the fold is plunging which suggests that there may be some association between the compressional crestal faults and the plunge of the fold. The thrust/reverse faults divide the crest of the fold into numerous fault slices. Each slice may have an apparent fold culmination. Following the erosion that has taken place after the folding, the western nose of the Waterman structure therefore appears to have multiple fold crests (Figure 1).
- The *eastern* nose of the structure also contains a high frequency of faults. Here, two main fault sets appear to dominate. They are the thrust/reverse faults trending parallel to the fold crest and east-west trending faults which are interpreted as right lateral shears. The fracture density appears to increase as the fold plunges to the east and the axis rotates to the north.

Other faults occur on different trends in the mapped area. Many of these faults are smaller extensional faults on the flanks of the anticline, probably produced by regional unloading. Most of these faults do not reach the prospective crestal area.

In the southeast, a major east-west trending fault zone is mapped. The faults disappear below the superficial cover to the east and west of the outcrop. The fault zone may be the only outcrop of the main east-west thrust which controls the Waterman Anticline.

3.4.3 High-grade areas for fracture porosity

The three main controls on fracture porosity are thought to be:

- The intersection zones between syn-tectonic thrust/reverse faults along the crest of the fold and faults at approximately right angles to the fold caused by erosional unloading. Numerous intersection zones are mapped along the crest of the structure.
- The zone of high 'Gaussian' strain along the crest of the fold where the folded beds are changing dip. The high strain area is thought to form a strip about 1.5 kilometres wide along the crest of the anticline.
- Zones of increased fracturing due to non-cylindrical folding. The two plunging noses of the fold are non-cylindrical and are therefore more prospective than the central cylindrical section of the fold.

Figure 1 Apparent multiple crests, western nose, Waterhouse Anticline.

These three structural features are mapped on Enclosure 4. Zones where these three structural features coincide are considered to be the most prospective parts of the anticline. The air photograph maps suggest that the two plunging noses of the structure represent the main targets for fracture reservoirs.

- The prospective area on the **western nose** is about 15 kilometres long and 4 kilometres wide. Here, the axis of the fold is non-cylindrical as it both plunges and deviates to the northwest. In addition, fracture density is high. The fold-parallel thrust/reverse faults are particularly well represented. Two main high fracture zones are identified at W^1 and W^2. The two zones may actually represent a single fracture zone as the area in between is outcropping shale which tends to obscure the traces of the faults on the air photographs.
- Non-cylindrical folding, high Gaussian strain and high fracture densities also occur on the **eastern nose** of the fold. Two fracture intersection zones are identified at W^3 and W^4. W^4 represents intersecting thrust/reverse faults and east-west trending shears. Tonal patterns on the Landsat suggest that some alteration of the surface soils and outcrop is possible here. At W^3, two thrust/reverse faults are intersected by a northeast trending fault element.

A further four fracture intersection zones are mapped in the cylindrical central section of the fold which are not thought to be as prospective at the targets on the noses of the fold. The high fracture zones are listed and ranked on Table 2.

Table 2 Fracture reservoir targets, Waterhouse Anticline.

TARGET (See Enc. 4)	RANK	COMMENTS
W^4	1	High fracture density of two main fault sets on curved and plunging eastern fold nose. The best target based on the air photo mapping. Possible alteration of outcrop may relate to hydrocarbon seepage.
W^1	2	Zone of high fracture density on the curved and plunging western nose. Faults may consist mainly of one set.
W^2	3	Possible extension of the W1 high fracture density area. The crest-parallel faults dominate. Cross faults are sparse.
W^3	4	Minor fracture intersection zone on the eastern nose. This area favored by Magellan geologists.
W^8	5	Four minor fracture intersection zones in the cylindrical part of the Waterhouse fold. Probably less prospective than targets on the two noses.
W^7	6	
W^6	7	
W^5	8	

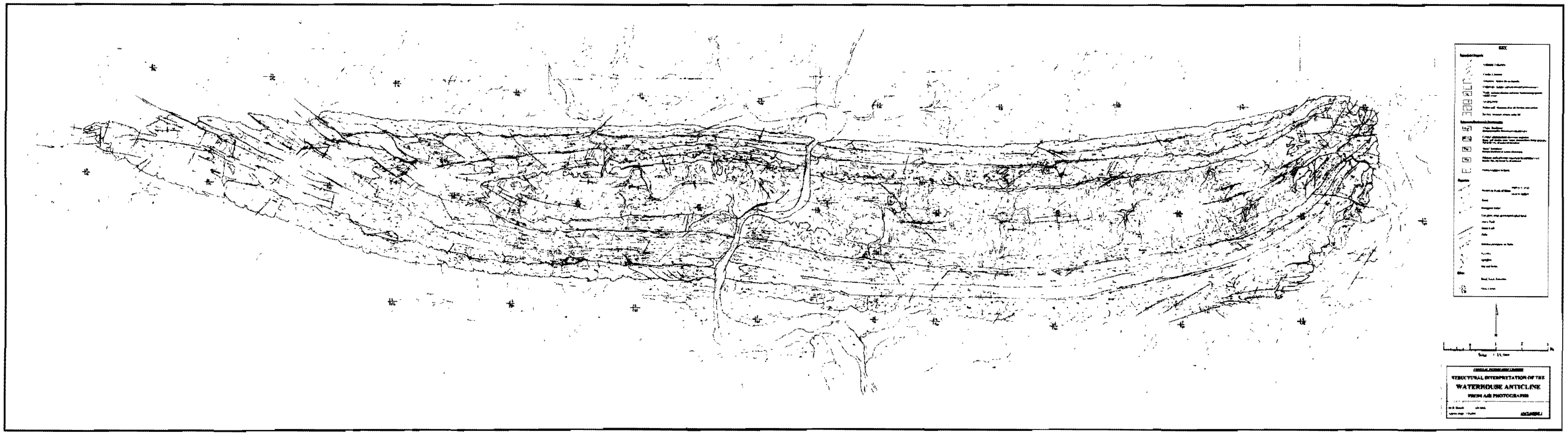
STRUCTURAL INTERPRETATION OF THE
WATERHOUSE ANTICLINE
FROM AIR PHOTOGRAPHS

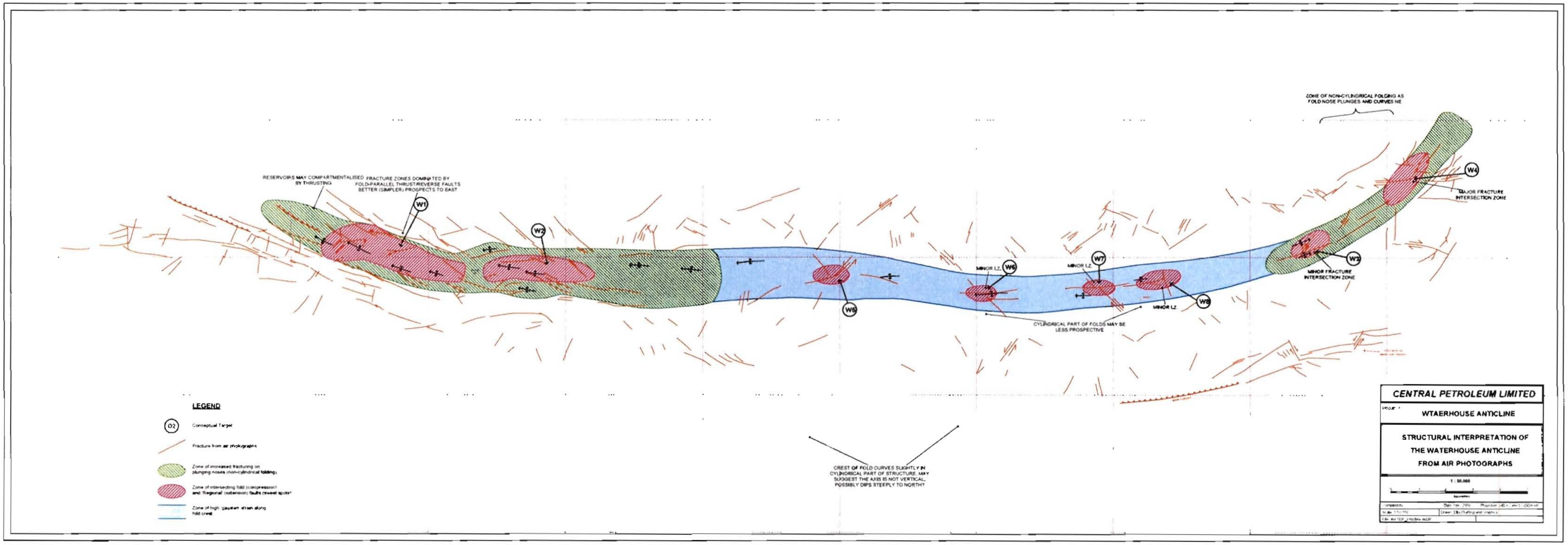
ZONE OF NON-CYLINDRICAL FOLDING AS
FOLD NOSE PLUNGES AND CURVES NE
RESERVOIRS MAY COMPARTMENTALISED
BY THRUSTING
FRACTURE ZONES DOMINATED BY
FOLD-PARALLEL THRUST/REVERSE FAULTS
BETTER (SIMPLER) PROSPECTS TO EAST
W1
W2
W5
MINOR I.Z.
W6
MINOR I.Z.
W7
W8
MINOR I.Z.
CYLINDRICAL PART OF FOLDS MAY BE
LESS PROSPECTIVE
W3
MINOR FRACTURE
INTERSECTION ZONE
W4
MAJOR FRACTURE
INTERSECTION ZONE
LEGEND
O2
Conceptual Target
Fracture from air photographs
Zone of increased fracturing on
plunging noses (non-cylindrical folding)
CREST OF FOLD CURVES SLIGHTLY IN
CYLINDRICAL PART OF STRUCTURE. MAY
SUGGEST THE AXIS IS NOT VERTICAL,
POSSIBLY DIPS STEEPLY TO NORTH?
CENTRAL PETROLEUM LIMITED
WTAERHOUSE ANTICLINE
STRUCTURAL INTERPRETATION OF
THE WATERHOUSE ANTICLINE
FROM AIR PHOTOGRAPHS
1 : 50,000

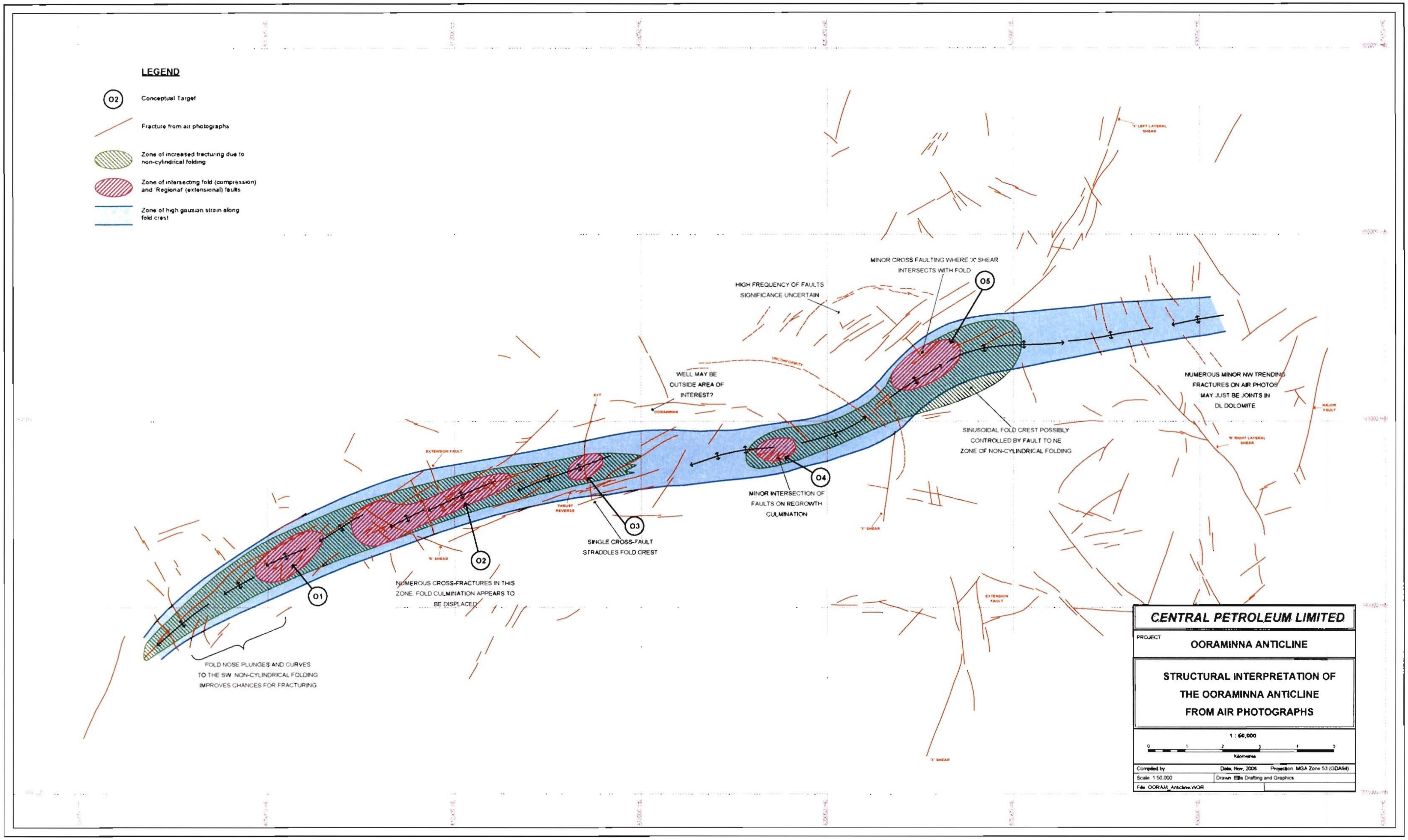

LEGEND
O2 Conceptual Target
Fracture from air photographs
Zone of increased fracturing due to non-cylindrical folding
Zone of intersecting fold (compression) and 'Regional' (extensional) faults
Zone of high gaussian strain along fold crest
MINOR CROSS FAULTING WHERE 'X' SHEAR INTERSECTS WITH FOLD
HIGH FREQUENCY OF FAULTS SIGNIFICANCE UNCERTAIN
WELL MAY BE OUTSIDE AREA OF INTEREST?
NUMEROUS MINOR NW TRENDING FRACTURES ON AIR PHOTOS MAY JUST BE JOINTS IN DL DOLOMITE
SINUSOIDAL FOLD CREST POSSIBLY CONTROLLED BY FAULT TO NE ZONE OF NON-CYLINDRICAL FOLDING
MINOR INTERSECTION OF FAULTS ON REGROWTH CULMINATION
SINGLE CROSS-FAULT STRADDLES FOLD CREST
NUMEROUS CROSS-FRACTURES IN THIS ZONE. FOLD CULMINATION APPEARS TO BE DISPLACED
FOLD NOSE PLUNGES AND CURVES TO THE SW. NON-CYLINDRICAL FOLDING IMPROVES CHANCES FOR FRACTURING
O1
O2
O3
O4
O5
CENTRAL PETROLEUM LIMITED
PROJECT
OORAMINNA ANTICLINE
STRUCTURAL INTERPRETATION OF THE OORAMINNA ANTICLINE FROM AIR PHOTOGRAPHS
1 : 60,000
0 1 2 3 4 5
Kilometres
Compiled by
Date. Nov. 2006
Projection MGA Zone 53 (GDA94)
Scale 1:50,000
Drawn Ellis Drafting and Graphics
File OORAM_Anticline.WOR

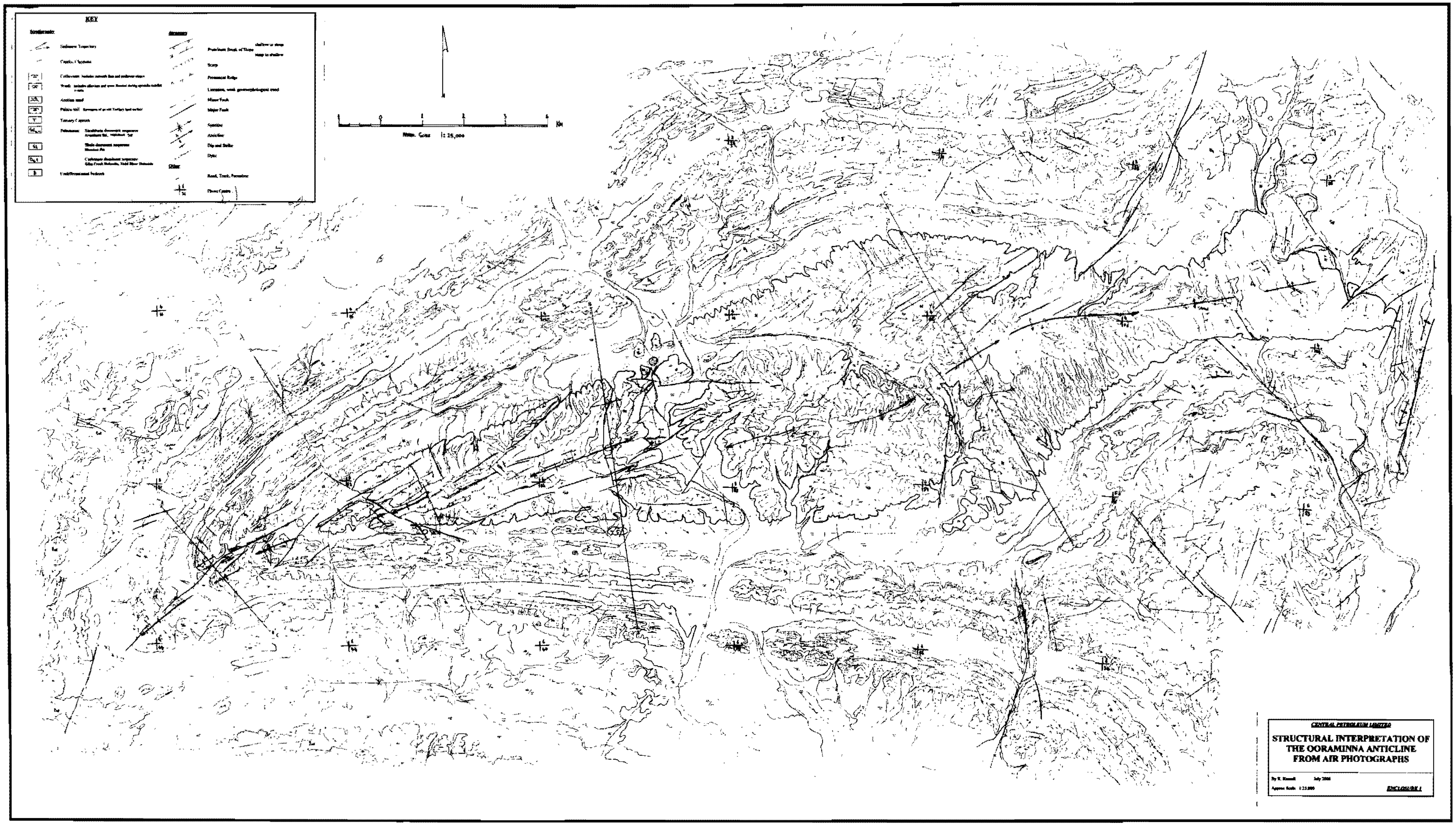
KEY
Scarp
Prominent Ridge
Minor Fault
Major Fault
Syncline
Anticline
Dip and Strike
Dyke
Other
Photo Centre
1:25,000
CENTRAL PETROLEUM LIMITED
STRUCTURAL INTERPRETATION OF THE OORAMINNA ANTICLINE FROM AIR PHOTOGRAPHS
ENCLOSURE 1

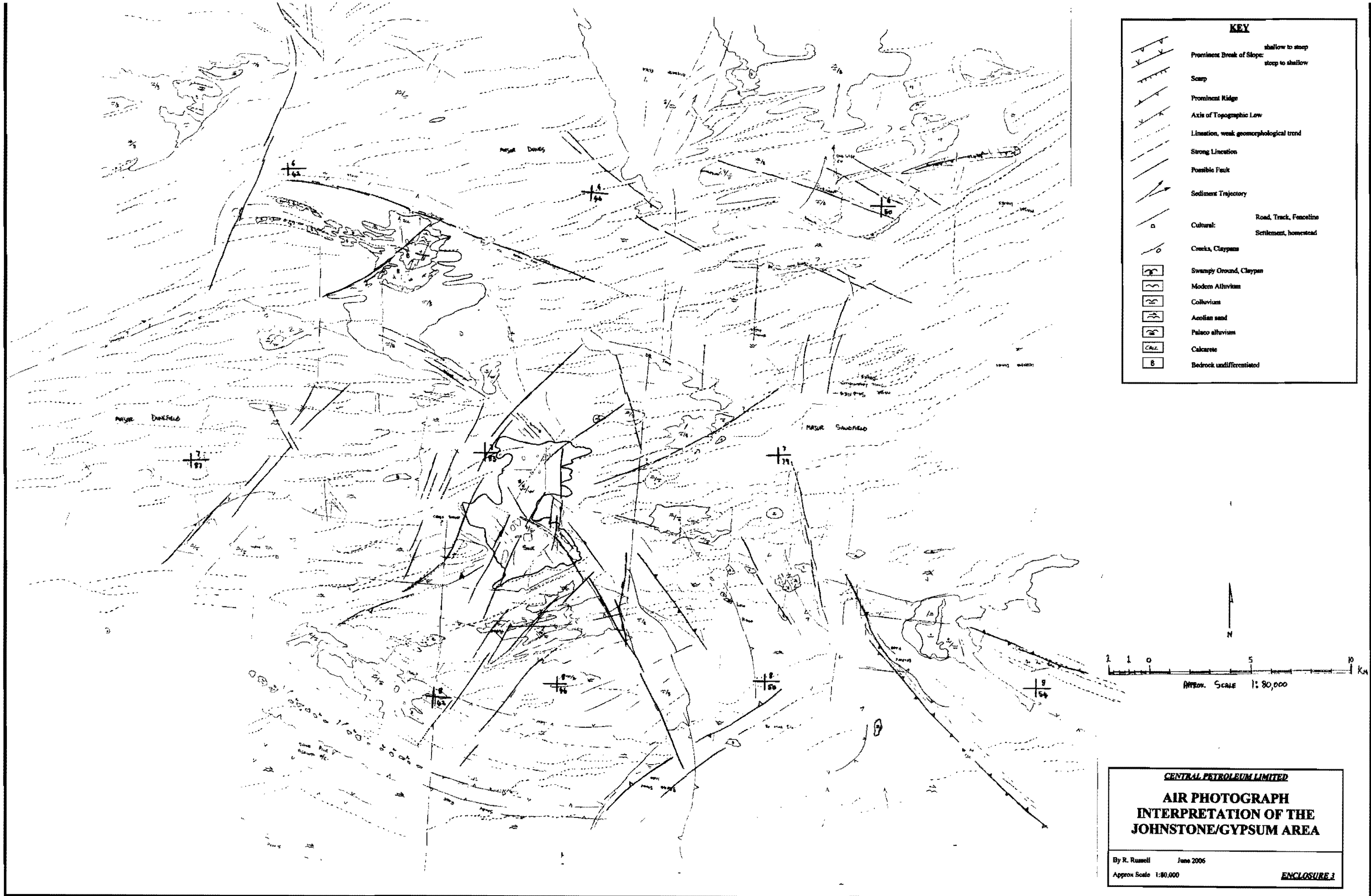

CENTRAL PETROLEUM LIMITED

AIR PHOTOGRAPH INTERPRETATION OF THE JOHNSTONE/GYPSUM AREA

By R. Russell June 2006

Approx Scale 1:80,000 ***ENCLOSURE 3***

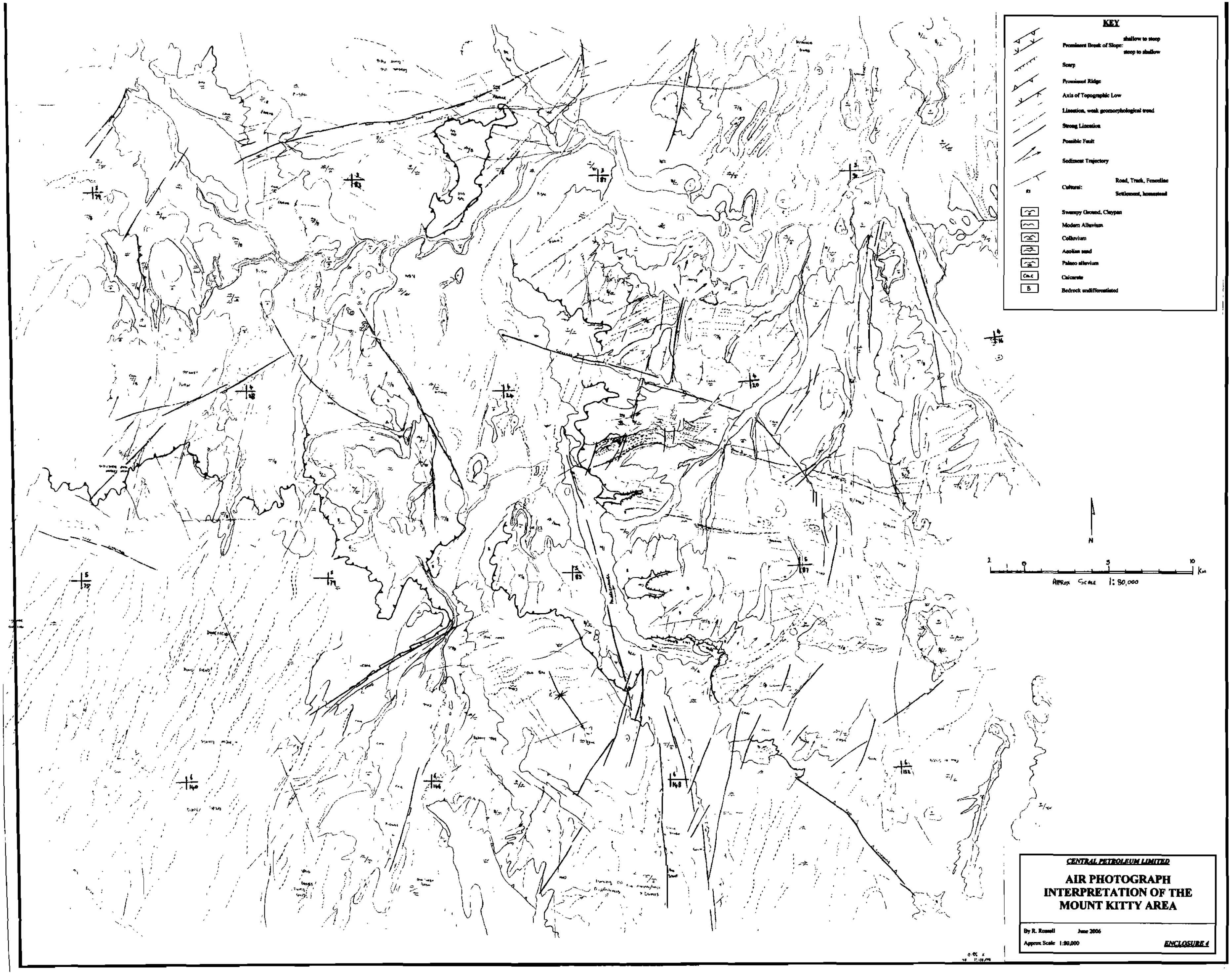
KEY
Prominent Break of Slope: shallow to steep
steep to shallow
Scarp
Prominent Ridge
Axis of Topographic Low
Lineation, weak geomorphological trend
Strong Lineation
Possible Fault
Sediment Trajectory
Cultural: Road, Track, Fenceline
Settlement, homestead
Swampy Ground, Claypan
Modern Alluvium
Colluvium
Aeolian sand
Palaeo alluvium
CALC
Calcrete
B
Bedrock undifferentiated
N
2 0 5 10 Km
Approx Scale 1:80,000
CENTRAL PETROLEUM LIMITED
AIR PHOTOGRAPH INTERPRETATION OF THE MOUNT KITTY AREA
By R. Russell June 2006
Approx Scale 1:80,000
ENCLOSURE 4